HHS Public Access

Author manuscript

J Inorg Biochem. Author manuscript; available in PMC 2016 August 25.

Published in final edited form as:

J Inorg Biochem. 2014 November ; 140: 39–44. doi:10.1016/j.jinorgbio.2014.06.015.

Cellular Uptake and Cytotoxicity of a Near-IR Fluorescent Corrole-TiO_2 Nanoconjugate

Carl M. Blumenfeld[†,‡], **Bryce F. Sadtler**[‡], **G. Esteban Fernandez**[#], **Lily Dara**[¶], **Cathie Nguyen**[§,δ], **Felix Alonso-Valenteen**[δ], **Lali Medina-Kauwe**[δ], **Rex A. Moats**[§], **Nathan S. Lewis**[†,‡], **Robert H. Grubbs**[‡], **Harry B. Gray**[†,‡,*], and **Karn Sorasaenee**[†,‡,§,*]

[†]Beckman Institute, California Institute of Technology, Pasadena, CA 91125 USA

[‡]Division of Chemistry and Chemical Engineering, California Institute of Technology, Pasadena, CA 91125 USA

[#]Cellular Imaging Core, The Saban Research Institute, Children's Hospital Los Angeles, Keck School of Medicine of USC, Los Angeles, CA 90027 USA

[¶]Division of Gastrointestinal and Liver Diseases, Department of Medicine, Keck School of Medicine of USC, Los Angeles, CA 90089 USA

[δ]Department of Biological Sciences, Cedars-Sinai Medical Center, David Geffen School of Medicine, University of California Los Angeles, Los Angeles, CA 90068 USA

[§]Translational Biomedical Imaging Laboratory, Department of Radiology, The Saban Research Institute, Children's Hospital Los Angeles, Keck School of Medicine of USC, Los Angeles, CA 90027 USA

Abstract

We are investigating the biological and biomedical imaging roles and impacts of fluorescent metallocorrole-TiO_2 nanoconjugates as potential near-infrared optical contrast agents *in vitro* in cancer and normal cell lines. The TiO_2 nanoconjugate labeled with the small molecule 2,17-bis(chlorosulfonyl)-5,10,15-tris(pentafluorophenyl)corrolato aluminum(III) (**1-Al**-TiO_2) was prepared. The nanoparticle **1-Al**-TiO_2 was characterized by transmission electron microscopy (TEM) and integrating-sphere electronic absorption spectroscopy. TEM images of three different samples of TiO_2 nanoparticles (bare, H_2O_2 etched, and **1-Al** functionalized) showed similarity in shapes and sizes with an average diameter of 29 nm for **1-Al**-TiO_2. Loading of **1-Al** on the TiO_2 surfaces was determined to be *ca*. 20–40 mg **1-Al**/g TiO_2. Confocal fluorescence microscopy (CFM) studies of luciferase-transfected primary human glioblastoma U87-Luc cells treated with the nanoconjugate **1-Al**-TiO_2 as the contrast agent in various concentrations were performed. The CFM images revealed that **1-Al**-TiO_2 was found inside the cancer cells even at low doses (0.02–2 μg/mL) and localized in the cytosol. Bioluminescence studies of the U87-Luc cells exposed to

Corresponding authors: Karn Sorasaenee, ksorasaenee@chla.usc.edu and Harry B. Gray, hbgray@caltech.edu.

various amounts of **1-Al**-TiO_2 showed minimal cytotoxic effects even at higher doses (2–2000 μg/mL) after 24 h. A similar observation was made using primary mouse hepatocytes (PMH) treated with **1-Al**-TiO_2 at low doses (0.0003–3 μg/mL). Longer incubation times (after 48 and 72 h for U87-Luc) and higher doses (> 20 μg/mL **1-Al**-TiO_2 for U87-Luc and > 3 μg/mL **1-Al**-TiO_2 for PMH) showed decreased cell viability.

Graphical Abstract

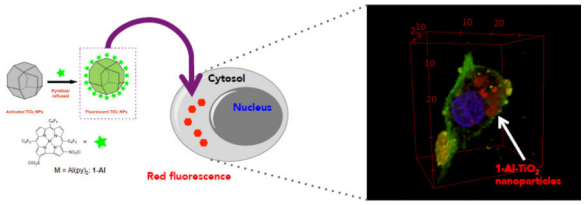

Synopsis for the graphic abstract

Fluorescence (shown in red) from the corrole nanoconjugate **1-Al**-TiO_2 internalized in the glioblastoma U87-Luc cell.

Keywords

Nanoconjugate; TiO_2 nanoparticle; Corrole; Fluorescence; Cytotoxic effect; Cellular uptake

1. Introduction

Small molecules, biomolecules, and biocompatible materials for molecular imaging have played an important role in recent advances in biomedical and drug development research[1–3]. Application of contrast agents is required by many imaging modalities and allows for better understanding of biochemical pathways, physiological processes, and disease pathologies[4–8]. Many small molecules and biomolecules that function as molecular imaging contrast agents have been utilized in both preclinical and clinical settings[9]. Recent efforts have focused on nanomaterials, a stark contrast to traditional small molecules and oligomers[10,11]. Aside from the sizes of these materials, including volumes and surface areas, which essentially provide a canvas for numerous small molecule labeling, they exhibit properties not generally found in either bulk materials or discreet molecules[12–14]. Examples of widely used and studied nanomaterials for biomedical imaging include quantum dots for optical imaging and superparamagnetic iron oxides for magnetic resonance imaging[10,11].

In our work, we have employed semiconductor nanoparticulate titanium(IV) oxide (TiO_2) covalently decorated with fluorescent corroles as a new class of optical imaging contrast agents for the study of cellular uptake and cytotoxic effects in cancer and normal cells. TiO_2, found in several different crystalline structures, such as rutile, anatase, and brookite, has been used in a number of contexts, including photocatalysis, dye-sensitized solar cells, and photochromic devices[15–19]. TiO_2 nanoparticles exhibit a wealth of intrinsic properties dependent upon several factors, including surface area, crystalline phase, and single

crystallinity. We have exploited the facile nature with which the surface can be decorated with corroles, which were selected as optical dyes. Many studies have shown that 5,10,15-trispentafluorophenyl corrole and its derivatives exhibit bright and robust fluorescence signals in the near-IR region ($\lambda_{em} \geq 600$ nm) and are therefore considered suitable candidates for optical imaging[20–23]. In addition, the chemical versatility of corroles, allowing for various metallation[24–26] and substitution[27,28] reactions, as well as their biological stability[29–31] make them attractive contrast agents.

Previously we reported the syntheses, spectroscopic characterizations, and spectral confocal fluorescence imaging results for a family of corrole-TiO_2 nanoconjugates, namely **1**-TiO_2, **1-Al**-TiO_2, and **1-Ga**-TiO_2[32]. The TiO_2 nanoparticle surfaces were covalently labeled with chlorosulfonated corroles through a sulfonic ester linkage (Scheme 1).

Because **1-Al**-TiO_2 exhibits the brightest fluorescence, consistent with the emission properties of related molecular Al corroles[26,32,33], we chose this nanoconjugate as a model to study cellular uptake and cytotoxic effects.

2. Experimental

2.1. Reagents and materials

Preparation of Al(III)tpfc$(SO_2Cl)_2$ (**1-Al**) and the nanoconjugate **1-Al**-TiO_2 was reported previously[32]. D-Luciferin potassium salt (Promega), Hoechst 34580 (Invitrogen™), Hoechst 33258 (Invitrogen™), Sytox Green (Invitrogen™), and FM® 1–43FX (Invitrogen™) were used as received according to the provider's instruction.

2.2. Physical Methods

Characterization of **1-Al** was performed by ^{1}H NMR, ^{19}F NMR, electronic absorption, and fluorescence spectroscopies, and was reported previously[32]. Surface characterization of **1-Al**-TiO_2 is outlined as follows.

2.2.1. Transmission Electron Microscopy—The morphologies of the TiO_2 nanoparticles before and after surface functionalization were imaged using a FEI Tecnai F30ST transmission electron microscope (TEM) operated at acceleration voltage of 300 kV. Images were recorded using a Gatan CCD camera. For TEM analysis, a small quantity of TiO_2 particles was dispersed in isopropyl alcohol (IPA) by sonication. The dispersions were drop-cast onto C-flat™ holey carbon films on a 200 mesh Cu TEM grid (Electron Microscopy Sciences).

2.2.2. Absorption Spectroscopy—Calculation of the corrole **1-Al**'s loading on the surface of TiO_2 was based on the absorbance values obtained from the integrating sphere electronic absorption measurements described as follows.

Thin film transflectance measurements were used to determine **1-Al** loading on the TiO_2 nanoparticles. Both H_2O_2-etched and **1-Al**-functionalized nanoparticles were dispersed in a polydimethylsiloxane (PDMS) polymer matrix. PDMS was chosen as it provides a transparent matrix for measuring the optical properties of porous solids[34]. The weights of

the TiO_2 nanoparticles, the PDMS base (Sylgard®184 silicone elastomer base from Dow Corning), and the curing agent (Sylgard®184 silicone elastomer curing agent from Dow Corning) are provided in Table A.1 in Appendix A. The nanoparticles were first dispersed in a minimal amount of IPA by sonication. The dispersion of TiO_2 nanoparticles in IPA was then mixed with the PDMS base and curing agent using a vortex mixer. The mixtures were cast into films onto quartz substrates and allowed to cure in air for 12 h followed by curing in a drying oven at 60° for 2 h.

Transflectance spectra of the H_2O_2-etched and **1-Al**-functionalized TiO_2 nanoparticle films were measured using a Cary 5000 UV-vis-NIR spectrometer from Agilent Technologies equipped with an integrating sphere (External DRA 1800), a PMT detector, a quartz-iodine lamp for the visible region (350–800 nm), and a deuterium lamp for the ultraviolet region (300–350 nm). Because the TiO_2 nanoparticles diffusely scattered the incident illumination, the PDMS films were placed in the center of the integrating sphere to collect both the transmitted, T, and the reflected, R, (including the spectrally reflected and diffusely scattered) light with the PMT detector. The transflectance measurements allowed for the absorbance, A, of the films to be determined by $A = -\log(T+R)$. The concentration, C, of **1-Al** within the PDMS films was then calculated using the Beer-Lambert law, $A = \varepsilon Cl$, where ε is the extinction coefficient of the dye and l is the film thickness (determined by profilometry, see below)[35– 37]. The absorbance values at 426 and 595 nm (corresponding to the Soret and Q bands of the dye, respectively) for the PDMS film containing the **1-Al**-functionalized TiO_2 nanoparticles, the estimated extinction coefficients of **1-Al** at these wavelengths, and the film thicknesses are provided in Table A.2 of Appendix A. The absorbance values for the PDMS film containing the non-functionalized, H_2O_2-etched TiO_2 nanoparticles at these wavelengths are also provided, which were subtracted from the absorbance values of the **1-Al**-functionalized TiO_2 nanoparticles. The **1-Al**-loading was determined to be 24 mg of **1-Al** per gram of TiO_2 based on the absorbance value of the Soret band and 38 mg of dye per gram of TiO_2 based on the absorbance value of the Q band.

Thickness profiles of the PDMS films were measured using a Bruker DektakXT stylus surface profilometer. The diameter of the diamond-tipped stylus was 2 μm and a weight of 1 mg was applied to the film. The stylus was scanned at a rate of 250 μm/s. The thickness profiles were used measure the average path length through the PDMS films during the transflectance measurements.

2.2.3. Hydrodynamic size and surface charge measurements—The mean particle size was determined by dynamic light scattering (DLS, Malvern ZEN 3600 Zetasizer Nano) measurements. Samples of **1-Al**-TiO_2 suspended in PBS pH 7.2 were pipetted into a low volume quartz cuvette with appropriate concentrations. At least nine measurements were performed for each sample. Each measurement comprised 20 runs with an average of 34,000 particle counts per second. The data represent the particle size distribution parameter, which reports the most frequent particle size in the sample accounting for the intensity fluctuations of larger particles. The particle intensity was computed using Zetasizer Software version 7.01 applying the Stokes-Einstein equation to correlate the change in the scattering intensity and particle movements. Plots showing the average size of the nanoparticle aggregates are shown in Figure A.1. The surface charge of **1-Al**-TiO_2 in PBS pH 7.2 was examined through

ζ potential measurements (Malvern ZEN 3600 Zetasizer Nano). The average ζ potential (Table A.3) was calculated from 20 measurements with 10–100 runs for each depending on the variation of the particles.

2.3. Cell Culture and Cell Viability Assay

Pathogen-free U87-LUC cell line (TSRI Small Animal Imaging and Research Laboratory) [38] was grown in a 75-mL flask in Dulbecco's Minumal Essential Medium (DMEM) in 5% CO_2 at 37 °C. The cell culture medium was supplemented with 10% fetal bovine serum (FBS) and 1% antibiotic primocin. The cell culture medium was replenished every 2 days and the cells were passaged once they reached 80% confluence. Primary mouse hepatocytes (PMH) were isolated and cultured as previously described[39].

For U87-Luc cell culture experiments, cells plated in an 8-chamber slide (Nunc™ Lab-Tek™, Thermo Scientific) were treated with **1-Al**-TiO_2 suspended in PBS over a range of 0.002 μg/mL to 2000 μg/mL. A primary stock solution (6.3 mg **1-Al**-TiO_2 in 1 mL PBS) was prepared. The primary stock solution was further diluted to prepare secondary and tertiary stock solutions. Various amounts of stock solutions were added to the 8-chamber glass slide plated with cells to give the aforementioned range of concentrations. The final volume of each chamber was 300 μL. After treatment, the treated cells and controls were incubated in the dark in 5% CO_2 at 37 °C for a period of 24, 48, and 72 h. The cells were imaged using a cooled IVIS® animal imaging system (Xenogen, Alameda, CA USA) linked to a PC running with Living Image™ software (Xenogen) along with IGOR (Wavemetrics, Seattle, WA, USA) under Microsoft® Windows® 2000. This system yielded high signal-to-noise images of luciferase signals emerging from the cells. Before imaging, 20 μL of 5 mg/mL luciferin in normal saline were added to each well. An integration time of 1 min with binning of 5 min was used for luminescent image acquisition. The signal intensity was quantified as the flux of all detected photon counts within each well using the LivingImage™ software package. All experiments were performed in triplicate.

For PMH cell culture experiments, the cells were plated in a 6-chamber slide (Falcon®, Primaria™). After 3 h, media was exchanged (DMEM-F12) and the cells were treated with **1-Al**-TiO_2 suspended in PBS over a range of 0.0003 to 300 μg/mL. A primary stock solution (6.3 mg **1-Al**-TiO_2 in 1 mL PBS) was prepared. The primary stock solution was further diluted to prepare secondary and tertiary stock solutions. Various amounts of stock solutions were added to the 6-chamber glass slide plated with cells to give the aforementioned range of concentrations. The final volume of each chamber was 2000 μL. After 24 or 48 h of treatment, cells were double stained with Hoechst 33258 (8 mg/mL) and Sytox Green (1 mM). Quantitation of total and necrotic cells (Sytox Green positive) was performed by counting cells in at least five different fields using ImageJ, as previously described[39]. All experiments were done in triplicate.

2.4. In Vitro Confocal Fluorescence Microscopy

The U87-Luc cells were seeded at 20,000 cells per well on an 8-chamber slide (Nunc™ Lab-Tek™, Thermo Scientific) and allowed to grow overnight. Cells were washed with PBS and were incubated in serum free media mixed 1:1 with **1-Al**-TiO_2 for 24, 48, and 72 h at 37 °C

over a concentration range similar to that of the U87-Luc cell viability assay (0.002 μg/mL to 2000 μg/mL). Cells were then washed 3× with PBS and stained with Hoechst 33258 and FM® 1–43FX stains. The stained cells were kept chilled on ice without fixation until just prior to imaging. Z-stacked images were acquired with an LSM 710 confocal system mounted on an AxioObserver Z.1 inverted microscope equipped with a 40×/1.2 C-APOCHROMAT water-immersion lens (Carl Zeiss Microimaging, Thronwood, NY). Two visible laser lines of 405 and 488 nm were used for fluorescence excitation. The Z-stacks were acquired with 0.5 μm slice intervals. The software ZEN 2010 was used for hardware control. To reduce blurring and noise in the raw images, they were processed with the 3D blind deconvolution algorithm of AutoQuant AutoDeblur software (Media Cybernetics, Silver Spring, MD) using the default settings for the laser scanning confocal modality. ZEN and Fiji ImageJ software[40] was employed to further process the deconvolved images.

3. Results and Discussion

3.1 Physical Characterization of 1-Al-TiO_2: TEM, DLS, and Surface Characterization

TEM images of TiO_2 (Figure 1) were taken before and after H_2O_2-etching and surface functionalization. The images established that the average particle size post-corrole functionalization is 29 nm with a standard deviation of 7 nm. These results were obtained through averaging over 44 particles. Absorption measurements of the particles embedded in a transparent polymer matrix, facilitated with the use of an integrating sphere to distinguish between absorption and diffuse scattering by the nanoparticles, indicated nearly identical absorption features in the molecular and conjugated species. These experiments afforded an approximate loading of **1-Al** on the surfaces of *ca*. 20–40 mg/g TiO_2 (Figure 2).

The hydrodynamic nature of **1-Al**-TiO_2 in PBS measured by the DLS method revealed great heterogeneity in size of the aggregates. While the average size of **1-Al**-TiO_2 in PBS was measured to be 200 nm in diameter, smaller and larger aggregates were observed (Appendix A). In addition, zeta (ζ) potential measurements of **1-Al**-TiO_2 in PBS exhibited moderate stability and revealed a negatively charged surface with a ζ potential of −27.4 (±1.25) mV at the concentration of 50 μg/mL.

3.2 Confocal Fluorescence Microscopy and Uptake of 1-Al-TiO_2 by U87-Luc Cells

Treatment of the luciferase-transfected glioblastoma cell U87-Luc with a wide range of **1-Al**-TiO_2 concentrations revealed internalization of these nanoconjugates over a period of 24, 48, and 72 h as shown by CFM (Figure 3). We also show the Z-stacked three-dimensional CFM images (Figure 4) of U87-Luc cells treated with 0.02 μg/mL of **1-Al**-TiO_2 for 48 and 72 h from three different perspectives.

The CFM images were taken after the cells were stained with nuclear and cell membrane dyes, and washed with media solution several times to remove unbound dyes and **1-Al**-TiO_2 nanoconjugates. The nucleus labeled with a Hoechst stain is colored blue (λ_{ex} = 405; λ_{em} = 460 nm), the membrane labeled with the dye FM® 1–43FX is colored green (λ_{ex} = 488; λ_{em} = 580 nm), and the nanoconjugate **1-Al**-TiO_2 is colored red (λ_{ex} = 405; λ_{em} = 634 nm).

While mechanisms of **1-Al**-TiO_2 uptake and localization into cells will be studied further, we propose that the **1-Al**-TiO_2 nanoconstruct is internalized through endocytosis, consistent with previous work[41–46]. We note that, based on confocal fluorescence imaging, the nanomaterial **1-Al**-modified TiO_2 appears to be suspended in the cytosol. This finding is consistent with the distribution pattern of TiO_2 nanoconjugates in HeLa cells in a previous study of 1D TiO_2 nanorods and nanoparticles labeled with fluorescein thiocyanate[43]. However, modified TiO_2 labeled with alizarin red S has been shown to have perinuclear localization in HeLa cells, in contrast to our observations with **1-Al**-TiO_2[41,42]. Recent studies involving uptake of other modified TiO_2 nanoparticles in various cell lines, such as mouse fibroblasts and osteoblasts, suggested cellular internalization and distribution of TiO_2 nanoparticles at the endosome/lysosome and in the cytoplasm, in accord with our findings[44,45]. We note that internalization of **1-Al**-TiO_2 into glioblastoma cells can be observed at very low concentrations (0.02–2 μg/mL).

3.3 Cytotoxicity in U87-Luc Cells

It is well documented that TiO_2 nanoparticles exhibit various degrees of cytotoxic activity upon photoactivation by UV-vis light due to formation of reactive oxygen species[43,44,46]. A study of water-soluble single-crystalline TiO_2 nanoparticles in melanoma A-375 cells revealed that in the absence of UV light the TiO_2 nanoparticles were essentially non-toxic and thus biocompatible[46]. However, upon irradiating these cells with UV light less than 20% of the melanoma cells survived at a TiO_2 concentration of 400 μg/mL. Therefore, in an attempt to understand the cytotoxic effects of the **1-Al**-TiO_2 conjugate independently of its phototoxic properties, we treated the glioblastoma cell U87-Luc in the absence of UV-vis irradiation with the same range of **1-Al**-TiO_2 concentrations as in the cell internalization studies (0.002–2000 μg/mL). The cells were incubated over a period of 24, 48, and 72 h prior to bioluminescence cell viability assays[38,47]. Based on the bioluminescence signal of the firefly luciferin from living U87-Luc cells, which is related to the level of cellular ATP, the cytotoxic assay showed that the nanoconjugate **1-Al**-TiO_2 had essentially no cytotoxic effect on the glioblastoma cells after 24 h of treatment (Figure 5) and, therefore, could be considered biocompatible. The cytotoxic effect became more apparent as the cells were exposed to the corrole-TiO_2 nanoparticles for extended periods of time at higher concentrations (> 200 μg/mL). For example, only *ca.* 65% and *ca.* 30% of the bioluminescence signal from the live cells was observed after 48-h and 72-h treatments at 2000 μg/mL, respectively. Our viability study of the U87-Luc cells treated with **1-Al**-TiO_2 was also consistent with a study performed on mouse fibroblast cells, using the MTT assay, showing that the cytotoxic effects of TiO_2 at various concentrations (3–600 μg/mL) were negligible after 24 h of treatment, whereas the 48-h treatment of these cells with the nanoparticle showed a decrease in cell viability at higher concentrations[44]. Another study on the cytotoxicity effect of unmodified 1D and 3D TiO_2 nanostructures on HeLa cells also showed that these nanoparticles were relatively nontoxic at concentrations up to 125 μg/mL in the absence of light[43].

3.4 Cytotoxicity in Primary Mouse Hepatocytes

Additionally, to determine the cytotoxic effect of the nanoconjugate **1-Al**-TiO_2 on non-cancerous cells, we treated primary mouse hepatocytes (PMH) with **1-Al**-TiO_2 at various concentrations (0.0003–300 μg/mL) for 24 and 48 h (Figure 6) in the absence of UV-vis irradiation. Similar to the results observed for cancerous U87-Luc cells, **1-Al**-TiO_2 was essentially nontoxic in non-cancerous PMH at up to 3 μg/mL after both 24 and 48 h of treatment. Only at higher concentrations did the proportion of the live PMH drop below 80%. We note that the PMH behaved similarly after 24-h and 48-h treatments with various doses of **1-Al**-TiO_2, suggesting that low **1-Al**-TiO_2 concentrations had minimal cytotoxic effects on the viability of these non-cancerous cells. The PMH were more susceptible to the cytotoxic effects of **1-Al**-TiO_2 than the U87-Luc cells; it is reasonable that non-cancerous cells, especially primary cells, would be less tolerant towards exogenous non-native agents[48,49]. Nonetheless, the intense fluorescence exhibited by **1-Al**[26,33] would allow for the potential use of the nanoconjugate **1-Al**-TiO_2 as an optical imaging agent observable by confocal fluorescence microscopy even at low concentrations (0.02–2 μg/mL) below the cytotoxic thresholds for both cancerous and non-cancerous cells.

4. Conclusions

In summary, we report detailed characterization of **1-Al**-TiO_2, a nanoconjugate that potentially could be used as a metal oxide nanoprobe for optical imaging, owing to intense fluorescence as well as its biocompatibility. The biological studies suggest that **1-Al**-TiO_2 is essentially nontoxic at concentrations up to 3 and 2000 μg/mL for normal mouse liver cells and glioblastoma U87-Luc cells, respectively, within the first 24 h of treatment. The PMH viability, however, dropped at higher concentrations (> 3 μg/mL) after 24-h and 48-h treatments and the U87-Luc cell viability also declined at higher concentrations (> 20 μg/mL) after 48-h and 72-h treatments. We also would like to note, for example, that comparable to our PMH cytotoxic assay over the concentration range for **1-Al**-TiO_2 of 0.0003–300 μg/mL, superparamagnetic iron oxide nanoparticle used in MRI was studied for their cytotoxicity in fetal stem cell lines over a low concentration range (5–35 μg/mL)[50]. Another example includes PDMAEMA-modified ZnO QDs functioning as contrast agents in monkey kidney cells over a concentration range of 50–800 μg/mL[51]. More importantly, our CFM studies demonstrated that the nanoconjugate **1-Al**-TiO_2 was internalized in U87-Luc cells even at a relatively low concentration (0.02 μg/mL). Although further detailed localization and internalization mechanism studies should be performed, our current work has revealed that there is random suspension of **1-Al**-TiO_2 in the cytosol even after 72-h treatment. Notably, the observation of near-IR fluorescence of **1-Al**-TiO_2 over a non-toxic concentration range (0.002–2000 μg/mL) in U87-Luc after 24-h treatment suggests that corrole-TiO_2 nanoconjugates could be very promising candidates for use as biological imaging agents.

Supplementary Material

Refer to Web version on PubMed Central for supplementary material.

Acknowledgments

We thank the CHLA Radiology Endowment Fund (K.S.), Sanofi (H.B.G.), Doheny Eye Institute (R.H.G.), and Beckman Institute Postdoctoral Fellowship (B.F.S.) for support. We also thank Anahit Hovsepyan, Seda Mkhitaryan, Vazgen Khankaldyyan, and Gevorg Karapetyan for help with the bioluminescence assays. Absorption measurements and profilometry were performed at the Molecular Materials Research Center, Beckman Institute, Caltech. We thank Carol M. Garland for assistance in TEM imaging. B.F.S. and N.S.L. acknowledge support from the "Light–Material Interactions in Energy Conversion" Energy Frontier Research Center funded by the US Department of Energy, Office of Science, Office of Basic Energy Sciences (DE-SC0001293).

Appendix A

Supplementary Data: Supplementary data to this article can be found online at http://www.sciencedirect.com/science/journal/01620134.

References

1. Willmann JK, van Bruggen N, Dinkelborg LM, Gambhir SS. Nat. Rev. Drug Discov. 2008; 7:591–607. [PubMed: 18591980]
2. Smith BA, Smith BD. Bioconjug. Chem. 2012; 23:1989–2006. [PubMed: 22989049]
3. Chow EK-H, Ho D. Sci. Transl. Med. 2013; 5:1–12.
4. Keren S, Zavaleta C, Cheng Z, de la Zerda A, Gheysens O, Gambhir SS. Proc. Natl. Acad. Sci. U. S. A. 2008; 105:5844–5849. [PubMed: 18378895]
5. Devaraj NK, Weissleder R, Hilderbrand SA. Bioconjug. Chem. 2008; 19:2297–2299. [PubMed: 19053305]
6. Mather S. Bioconjug. Chem. 2009; 20:631–643. [PubMed: 19086866]
7. Kelkar SS, Reineke TM. Bioconjug. Chem. 2011; 22:1879–1903. [PubMed: 21830812]
8. Wilson K, Homan K, Emelianov S. Nat. Commun. 2012; 3:1–10.
9. Winter PM, Caruthers SD, Kassner A, Harris TD, Chinen LK, Allen JS, Lacy EK, Zhang H, Robertson JD, Wickline SA, Lanza GM. Cancer Res. 2003; 63:5838–5843. [PubMed: 14522907]
10. Endres PJ, Paunesku T, Vogt S, Meade TJ, Woloschak GE. J. Am. Chem. Soc. 2007; 129:15760–15761. [PubMed: 18047347]
11. Xie J. Inorg. Chem. 2008; 47:5564–5566. [PubMed: 18540592]
12. Daniel M-C, Astruc D. Chem. Rev. 2004; 104:293–346. [PubMed: 14719978]
13. Wilcoxon JP, Abrams BL. Chem. Soc. Rev. 2006; 35:1162–1194. [PubMed: 17057844]
14. Murthy SK. Int. J. Nanomedicine. 2007; 2:129–141. [PubMed: 17722542]
15. Bavykin DV, Friedrich JM, Walsh FC. Adv. Mater. 2006; 18:2807–2824.
16. Albu SP, Ghicov A, Macak JM, Hahn R, Schmuki P. Nano Lett. 2007; 7:1286–1289. [PubMed: 17455983]
17. Macwan DP, Dave PN, Chaturvedi S, Mater J. Sci. 2011; 46:3669–3686.
18. O'Regan B, Gratzel M. Nature. 1991; 353:737–740.
19. Fujishima A, Honda K. Nature. 1972; 238:37–38. [PubMed: 12635268]
20. Gross Z, Galili N, Saltsman I. Angew. Chem. Int. Ed. 1999; 38:1427–1429.
21. Sankar J, Anand VG, Venkatraman S, Rath H, Chandrashekar TK. Org. Lett. 2002; 4:4233–4235. [PubMed: 12443066]
22. Tsai C-L, Chen J-C, Wang W-J. J. Med. Biol. Eng. 2001; 21:7–13.
23. Huang Y, Tang J, Swanson BG, Cavinato AG, Lin M, Rasco BA. Carbohydr. Polym. 2003; 53:281–288.
24. Bendix J, Dmochowski IJ, Gray HB, Mahammed A, Simkhovich L, Gross Z. Angew. Chemie Int. Ed. 2000; 39:4048–4051.
25. Weaver JJ, Sorasaenee K, Sheikh M, Goldschmidt R, Tkachenko E, Gross Z, Gray HB. J. Porphyrins Phthalocyanines. 2004; 08:76–81.

26. Sorasaenee K, Taqavi P, Henling LM, Gray HB, Tkachenko E, Mahammed A, Gross Z. J. Porphyrins Phthalocyanines. 2007; 11:189–197.
27. Mahammed A, Goldberg I, Gross Z. Org. Lett. 2001; 3:3443–3446. [PubMed: 11678678]
28. Saltsman I, Mahammed A, Goldberg I, Tkachenko E, Botoshansky M, Gross Z. J. Am. Chem. Soc. 2002; 124:7411–7420. [PubMed: 12071750]
29. Mahammed A, Gray HB, Weaver JJ, Sorasaenee K, Gross Z. Bioconjug. Chem. 2004; 15:738–746. [PubMed: 15264860]
30. Agadjanian H, Weaver JJ, Mahammed A, Rentsendorj A, Bass S, Kim J, Dmochowski IJ, Margalit R, Gray HB, Gross Z, Medina-Kauwe LK. Pharm. Res. 2006; 23:367–377. [PubMed: 16411149]
31. Agadjanian H, Ma J, Rentsendorj A, Valluripalli V, Hwang JY, Mahammed A, Farkas DL, Gray HB, Gross Z, Medina-Kauwe LK. Proc. Natl. Acad. Sci. U. S. A. 2009; 106:6105–6110. [PubMed: 19342490]
32. Blumenfeld CM, Grubbs RH, Moats RA, Gray HB, Sorasaenee K. Inorg. Chem. 2013; 52:4774–4776. [PubMed: 23611256]
33. Mahammed A, Gross Z, Inorg J. Biochem. 2002; 88:305–309.
34. Kelzenberg MD, Boettcher SW, Petykiewicz Ja, Turner-Evans DB, Putnam MC, Warren EL, Spurgeon JM, Briggs RM, Lewis NS, Atwater HA. Nat. Mater. 2010; 9:239–244. [PubMed: 20154692]
35. Ceriotti L, Weible K, De Rooij NF, Verpoorte E. Microelectron. Eng. 2003; 67–68:865–871.
36. Shahzad N, Pugliese D, Lamberti A, Sacco A, Virga A, Gazia R, Bianco S, Shahzad MI, Tresso E, Pirri CF. J. Phys. Conf. Ser. 2013; 439:1–12.
37. Ryu D, Loh KJ, Ireland R, Karimzada M, Yaghmaie F, Gusman AM. Smart Struct. Syst. 2011; 8:471–486.
38. Burgos JS, Rosol M, Moats RA, Khankaldyyan V, Kohn DB, Nelson MD Jr, Laug WE. Biotechniques. 2003; 34:1184–1188. [PubMed: 12813886]
39. Feng G, Kaplowitz N, Clin J. Invest. 2000; 105:329–339.
40. Schindelin J, Arganda-Carreras I, Frise E, Kaynig V, Longair M, Pietzsch T, Preibisch S, Rueden C, Saalfeld S, Schmid B, Tinevez J-Y, White DJ, Hartenstein V, Eliceiri K, Tomancak P, Cardona A. Nat. Methods. 2012; 9:676–682. [PubMed: 22743772]
41. Thurn KT, Arora H, Paunesku T, Wu A, Brown EMB, Doty C, Kremer J, Woloschak G. Nanomedicine. 2011; 7:123–130. [PubMed: 20887814]
42. Blatnik J, Luebke L, Simonet S, Nelson M, Price R, Leek R, Zeng L, Wu A, Brown EMB. Microsc. Microanal. 2012; 18:134–142. [PubMed: 22214568]
43. Chen J, Zhou H, Santulli AC, Wong SS. Chem. Res. Toxicol. 2010; 23:871–879. [PubMed: 20408587]
44. Jin C-Y, Zhu B-S, Wang X-F, Lu Q-H. Chem. Res. Toxicol. 2008; 21:1871–1877. [PubMed: 18680314]
45. Cai K, Hou Y, Hu Y, Zhao L, Luo Z, Shi Y, Lai M, Yang W, Liu P. Small. 2011; 7:3026–3031. [PubMed: 21919195]
46. Seo J, Chung H, Kim M, Lee J, Choi I, Cheon J. Small. 2007; 3:850–853. [PubMed: 17385208]
47. Gould SJ, Subramani S. Anal. Biochem. 1988; 175:5–13. [PubMed: 3072883]
48. Li AP. Primary Hepatocyte Cultures as an in Vitro Experimental Model for the Evaluation of Pharmacokinetic Drug–Drug Interactions. Adv. Pharmacol. 1997:103–130. [PubMed: 9342174]
49. Hengstler JG, Utesch D, Steinberg P, Ringel M, Swales N, Biefang K, Platt KL, Diener B, Böttger T, Fischer T, Oesch F. Drug Metab. Rev. 2000; 32:81–118. [PubMed: 10711408]
50. Zhang P, Liu W. Biomaterials. 2010; 31:3087–3094. [PubMed: 20096454]
51. Diana V, Bossolasco P, Moscatelli D, Silani V, Cova L. PLoS ONE. 2013; 8:e78435. [PubMed: 24244310]

Highlights

- We examined a potential use of the corrole nanoconjugate **1-Al**-TiO_2 as an optical imaging contrast.
- **1-Al**-TiO_2 showed biocompatibility in both primary mouse hepatocyte and the glioblastoma U87-Luc.
- **1-Al**-TiO_2 was internalized by U87-Luc cells even after a long-term treatment (72 h).
- **1-Al**-TiO_2 showed intense near-IR fluorescence inside U87-Luc cells even at low doses of treatment (0.02–2 μg/mL)
- We reported detailed characterization of **1-Al**-TiO_2, including its hydrodynamic size, surface charge, and corrole loading.

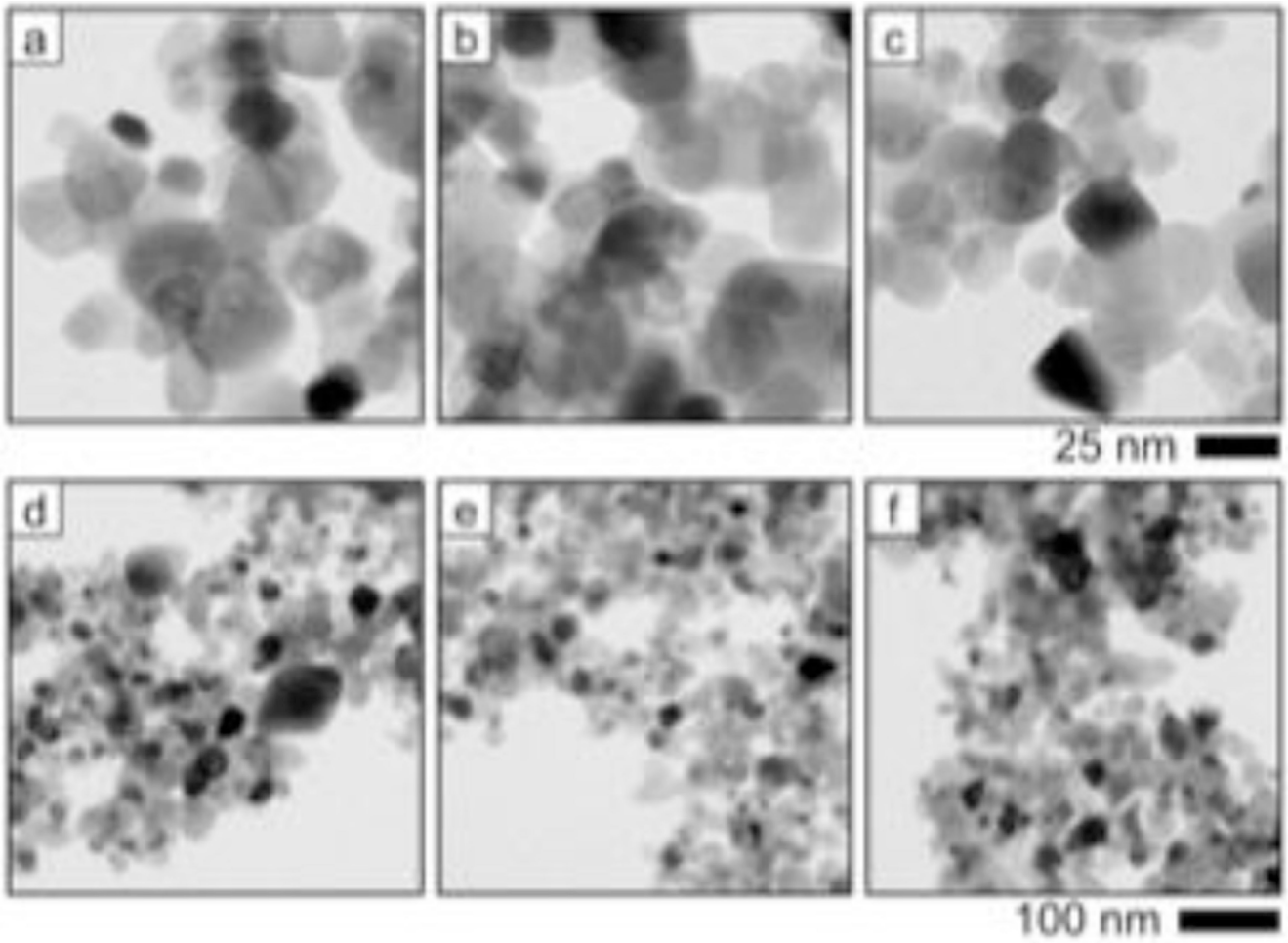

Figure 1.

TEM images of TiO_2 nanoparticles before and after dye-functionalization. Images of the initial TiO_2 nanoparticles (a and d). Images of the nanoparticles after H_2O_2-etching (b and e). Images of the nanoparticles after **1-Al** functionalization (c and f). The top scale bar refers to images a, b, and c and the bottom scale bar refers to images d, e, and f.

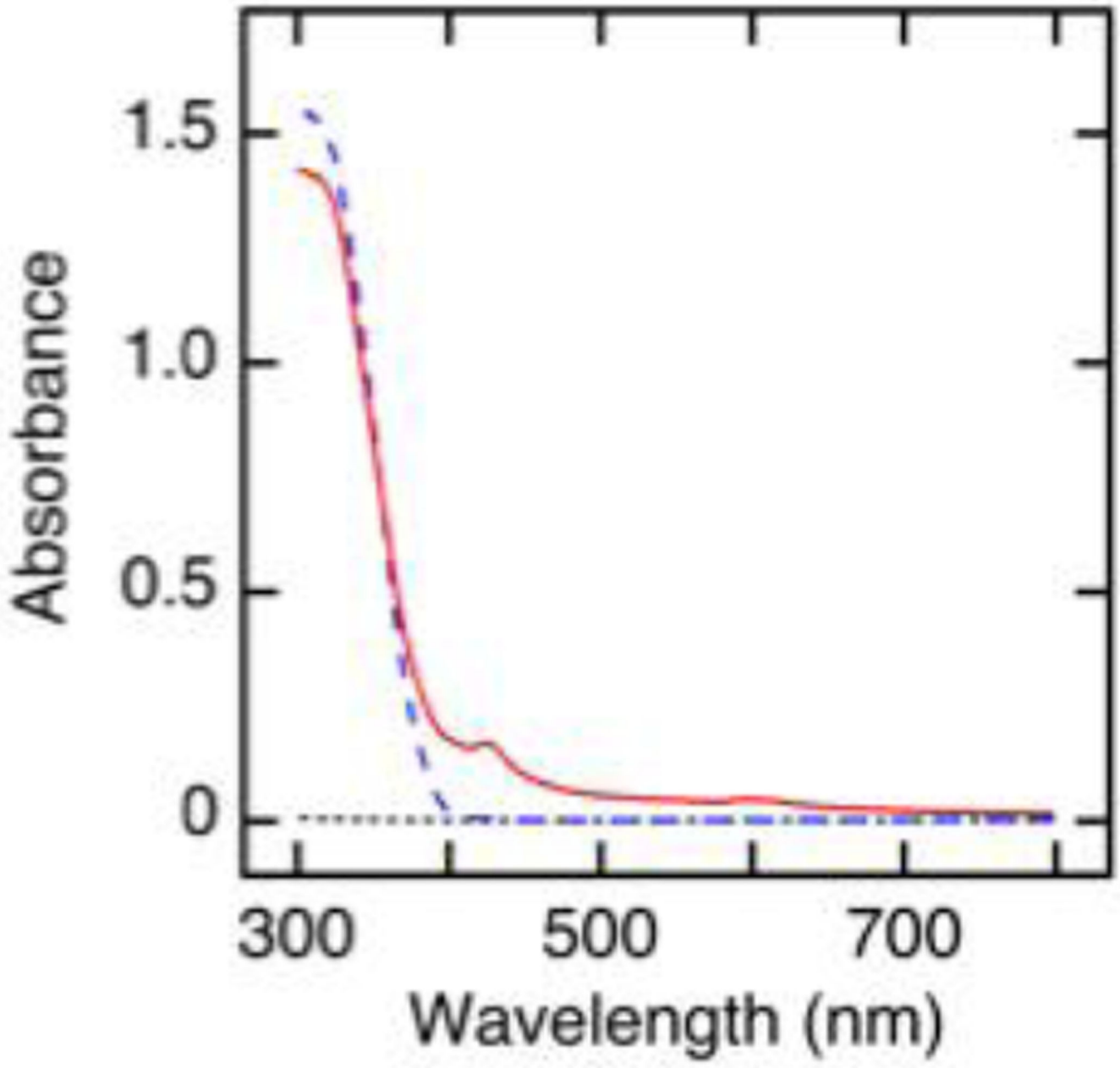

Figure 2.

Absorbance spectra of H_2O_2-etched TiO_2 nanoparticles embedded in a PDMS polymer matrix before (blue, long dashed line) and after 1-Al functionalization (red, solid line), as well as the absorption spectrum of PDMS on quartz (black, short dashed line). The absorption spectra were measured in transflectance mode where both transmitted and reflected lights were collected employing an integrating sphere.

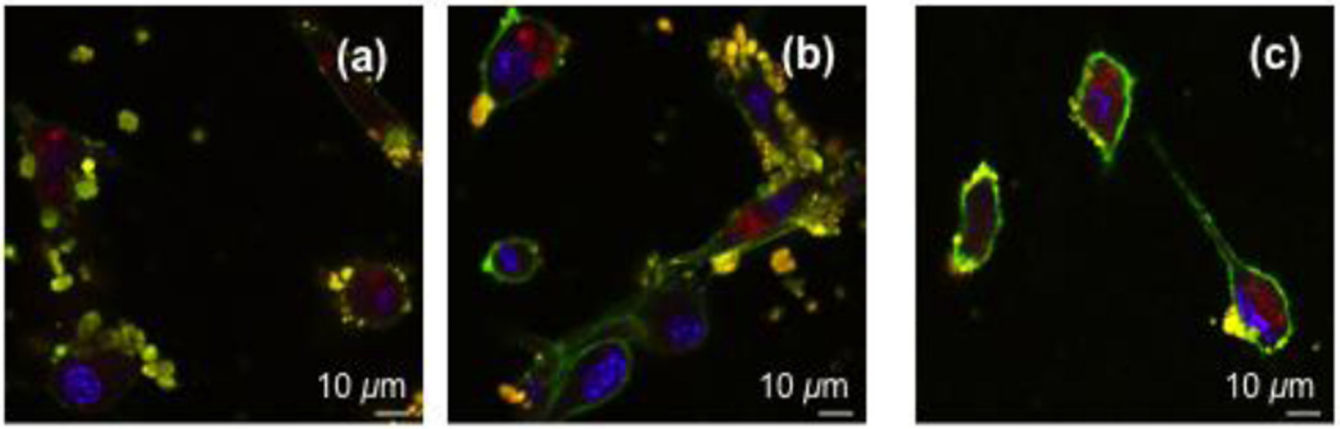

Figure 3.

CFM images of U87-Luc cells incubated with 0.02 μg/mL **1-Al**-TiO_2 (red) for 24 h (a), 48 h (b), and 72 h (c) and stained with dyes to mark the membrane (green) and nucleus (blue).

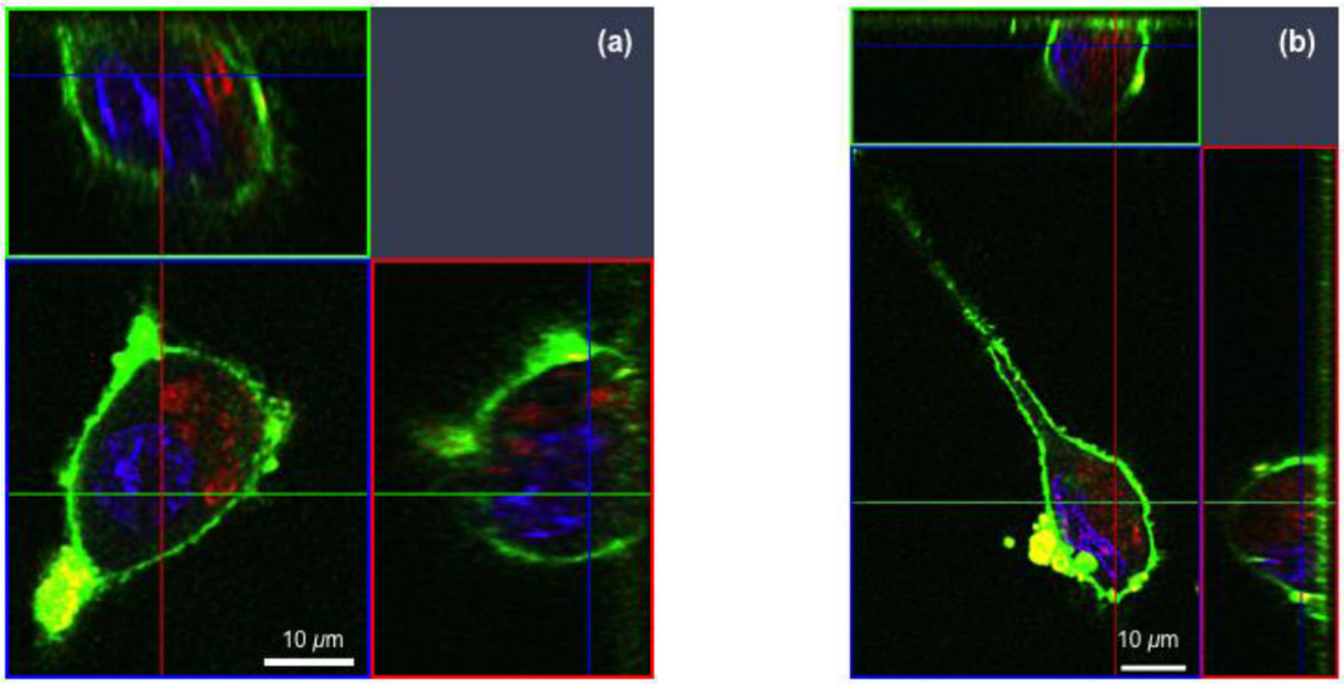

Figure 4.

Z-stacked CFM images of individual U87-Luc cells taken at 0.5-μm z-slice intervals from top to bottom after **(a)** 48 h and **(b)** 72 h of treatment with 0.02 μg/mL **1-Al**-TiO_2.

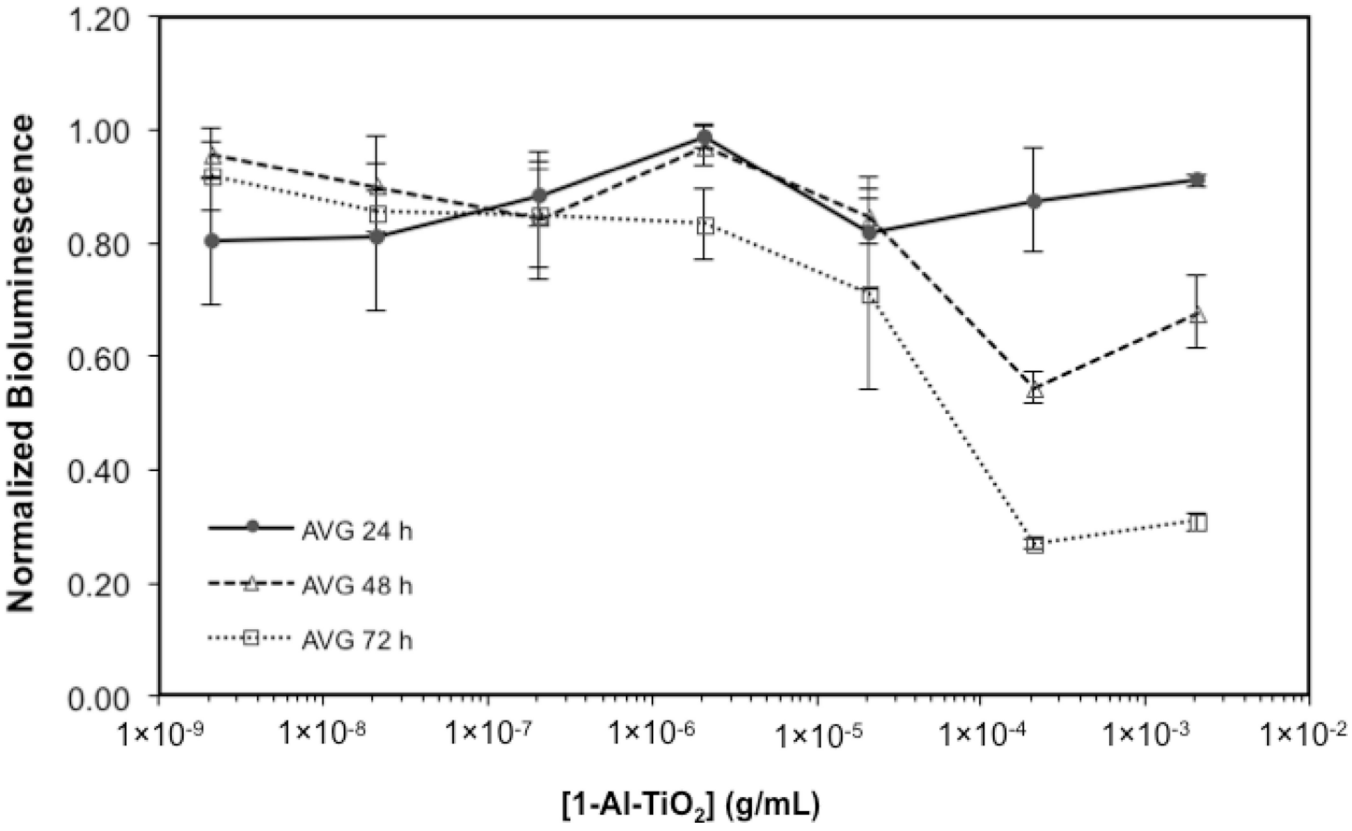

Figure 5.

Cell viability plot of U87-Luc cells treated by **1**-**Al**-TiO_2 at various concentrations (0.002–2000 μg/mL) using a bioluminescence assay.

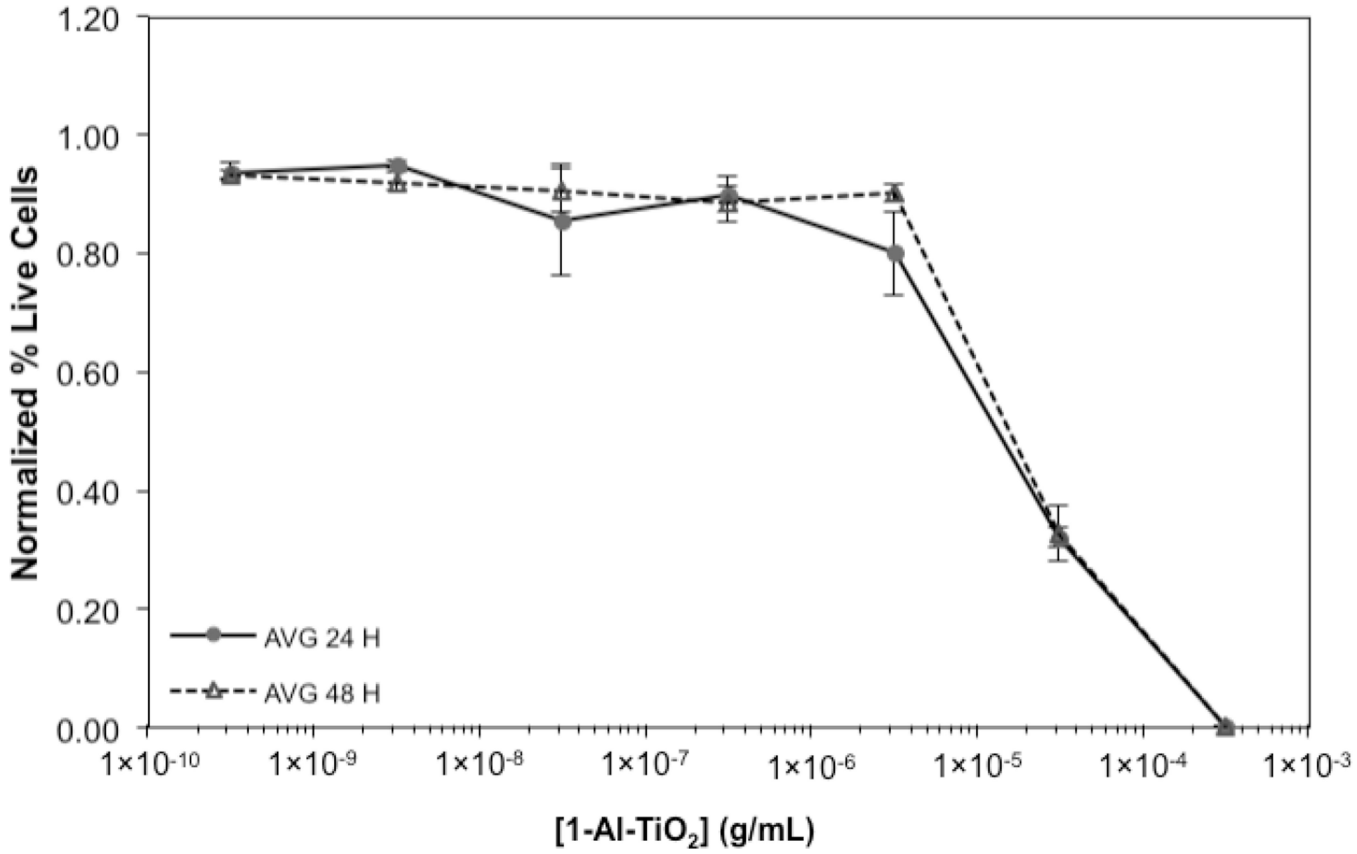

Figure 6.

Cell viability plot of PMH treated with **1-Al**-TiO_2 at various concentrations (0.0003–300 μg/mL) using a Syntox Green live-dead assay.

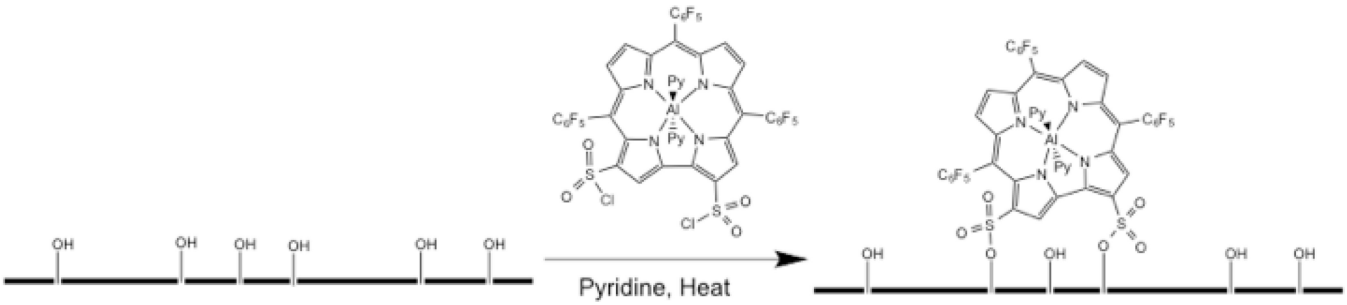

Scheme 1.

TiO_2 surface labeling with **1-Al** forming sulfonic ester linkages between the corrole and the surface.